Adsorption (2014) 20:453–463
DOI 10.1007/s10450-013-9570-z

Adsorption of carbon dioxide-methane mixtures in porous carbons: effect of surface chemistry

Pierre Billemont · Benoit Coasne · Guy De Weireld

Received: 6 May 2013 / Accepted: 29 August 2013 / Published online: 28 September 2013

Abstract A combined experimental and molecular simulation study of the coadsorption of CO_2 and CH_4 in porous carbons is reported. We address the effect of surface chemistry by considering a numerical model of disordered porous carbons which has been modified to include heterochemistry (with a chemical composition consistent with that of the experimental sample). We discuss how realistic the numerical sample is by comparing its pore size distribution (PSD), specific surface area, porous volume, and porosity with those for the experimental sample. We also discuss the different criteria used to estimate the latter properties from a geometrical analysis. We demonstrate the ability of the MP method to estimate PSD of porous carbons from nitrogen adsorption isotherms. Both the experimental and simulated coadsorption isotherms resemble those obtained for pure gases (type I in the IUPAC classification). On the other hand, only the porous carbon including the heterogroups allows simulating quantitatively the selectivity of the experimental adsorbent for different carbon dioxide/methane mixtures. This result shows that taking into account the heterochemistry present in porous carbons is crucial to represent correctly adsorption selectivities in such hydrophobic samples. We also show that the adsorbed solution theory describes quantitatively the simulated and experimental coadsorption isotherms without any parameter adjustment.

Keywords Carbon dioxide · Methane · Porous carbons · Mixtures

P. Billemont · G. De Weireld (✉)
Thermodynamics Department, Faculté Polytechnique, Université de Mons (UMons), 20 Place du Parc, 7000 Mons, Belgium
e-mail: guy.deweireld@umons.ac.be

B. Coasne (✉)
Institut Charles Gerhardt Montpellier (ICGM), UMR 5253 CNRS/ENSCM/Université de Montpellier II, 8 rue de l'Ecole Normale, 34296 Montpellier, France
e-mail: coasne@mit.edu

B. Coasne
MultiScale Material Science for Energy and Environment, CNRS/MIT (UMI 3466), 77 Massachusetts Avenue, Cambridge, MA 02139, USA

B. Coasne
Department of Civil and Environmental Engineering, Massachusetts Institute of Technology, 77 Massachusetts Avenue, Cambridge, MA 02139, USA

1 Introduction

Many research efforts have been devoted the last decade to foster carbon dioxide capture and storage (CCS) (Metz et al. 2005; Aaron and Tsouris 2005). Among solutions being considered, CO_2 storage in geological media such as oil and gas reservoirs, deep saline formations, or unminable coal beds are promising routes which have received considerable attention. Other solutions such as storage in nanoconfined solvents, for which "oversolubility" effects have been reported (Ho et al. 2011; Clauzier et al. 2012), are also receiving increasing attention. From an industrial point of view, a conceivable process would be to store supercritical CO_2 in unminable coal seams as it might, in the same time, provoke the liberation of methane that is naturally stored in these coal seams. While the latter process, which is referred to as enhanced coal bed methane (ECBM) is already in use in countries such as Canada, Australia, China, and India, fundamental and practical aspects still need to be understood and developed in order to enhance the recovery process. For instance, important

issues related to the adsorption mechanism, storage capacity, diffusion, permeability, swelling, etc. need to be solved and better understood to improve the process.

As far as swelling is concerned, several experimental and simulation studies have addressed the coupling between adsorption and volume strain of coal (Cui et al. 2007; Chen et al. 2012). Recently, poromechanics constitutive equations have been derived to describe swelling or shrinkage of microporous solids upon gas adsorption (Brochard et al. 2012a). The latter approach used to predict coal swelling upon CH_4 or CO_2 adsorption was found to be in good agreement with available experimental data (Brochard et al. 2012b). Another important issue relevant to CO_2 storage and CH_4 recovery in coals concerns the effect of the presence of adsorbed water, which cannot be avoided owing to the partial hydrophilic nature of the samples (White et al. 2005; Mazzotti et al. 2009). While most experiments have been performed on dry samples (Busch et al. 2004; Bae and Bhatia 2006; Ottiger et al. 2006; Day et al. 2008; Gensterblum et al. 2010), several authors have considered CO_2 or CH_4 adsorption on moisture-equilibrated coals (Hildenbrand et al. 2006; Goodman et al. 2007). Recenlty, we have reported a joint experimental and molecular simulation study on the adsorption of carbon dioxide and methane in activated carbons in the presence of water (Billemont et al. 2011; Billemont et al. 2013); both the experimental and simulated data show a linear decrease in the methane and carbon dioxide adsorbed amount upon increasing the number of adsorbed water molecules (on the other hand, we found that water does not affect the pore filling mechanism as the shape of the adsorption isotherm and the pressure at which the maximum CH_4 or CO_2 adsorbed amount is reached are nearly insensitive to the water content).

The aim of the present work is to investigate in details the role of surface chemistry on the adsorption of carbon dioxide/methane mixtures in porous carbons. Both experimental measurements and Grand Canonical Monte Carlo (GCMC) simulations are used to determine coadsorption isotherms at 318.15 K. Experiments are performed for a Filtrasorb 400 activated carbon, which constitutes a first step towards considering real coal samples. While being a simpler system, Filtrasorb 400 has a chemical composition and microporous structure comparable to those of natural coals. The molecular simulations are performed for a disordered porous carbon (Jain et al. 2005) which has been modified by Billemont et al. to include heterogroups (CH, COH, etc.) and, hence, better account for the chemical composition of real samples (Billemont et al. 2013). We note that other molecular models of coal, which take into account chemical heterogeneities, have been reported in the literature (Tambach et al. 2009; Tenney and Lastoskie 2006). Molecular models of coals have been recently reviewed (Mathews et al. 2011; Mathews and Chaffee 2012).

2 Experimental and computational methods

2.1 Experimental methods

The experimental sample Filtrasorb 400 (F400) is an activated carbon of Calgon Carbon Corporation which was kindly supplied by Chemviron Carbon GmbH, Germany. It is mainly composed of about 90 wt% carbon, 6 wt% oxygen, and 0.2 wt% hydrogen. F400 used in the present work has been described in details in a previous paper (Gensterblum et al. 2009). The sample was dried at 473 K for 24 h under secondary vaccum prior to performing the experiments.

2.1.1 Nitrogen adsorption

Nitrogen sorption isotherm at 77 K was performed on the F400 activated carbon using an automatic manometric sorption analyser BELSORP-max marketed by Bel Japan Inc. The adsorbents were placed in an adsorption cell and the adsorbates were dosed. The pressure change was monitored and the adsorbed amount was calculated by a mass balance on the gas phase before and after adsorption when the equilibrium was reached.

2.1.2 CO_2–CH_4 sorption measurements

The principle of volumetric co-adsorption measurements (Lewis et al. 1950; Kaul 1987) is based on classic pure compound manometric apparatus. In this home-built apparatus, a cylinder piston provides a substitute of the "classic" cell which enables changing the total volume in order to fix the pressure on a set point value during adsorption (Heymans et al. 2011). It allows the measurement of isobaric and isotherm mixture adsorption equilibria in a range of pressures from 100 to 3300 kPa and for temperatures from 298 to 353 K. A circulation pump is used to homogenize the mixture and a gas chromatograph, coupled with a thermal conductivity detector, provided by Agilent (GC 6850), allows determining the gas mole fraction of each component in the mixture. The pressure transmitter, provided by MKS (BARATRON® 627B 0—3300 kPa), allows measuring pressures with an accuracy of 0.12 % of the reading value. The pure gases (provided by Praxair, Belgium) are introduced one by one in the installation without going through the adsorption cell. We considered different carbon dioxide/methane mixtures with the following molar compositions: 75–25, 50–50, and

25–75 %. We performed measurements at 318.15 K and at different pressures.

Before and after adsorption, when the equilibrium is reached (checked by constant values of temperature, volume, and composition), the pressure, the temperature, and the volume values are recorded; finally the gas composition is measured by at least five chromatographic analyses. Knowing the total installation volume before and after adsorption, the mole number of each component in the gas phase before and after adsorption can be calculated thanks to a mixture equation of state (Kunz and Wagner 2012). The difference between the mole number in the gas phase before and after adsorption allows determining the adsorbed amounts. The adsorbent is then outgassed before starting the procedure with a new mixture.

The CO_2 adsorption selectivity is defined by the following expression:

$$S_{CO_2,CH_4} = \frac{x_{CO_2}/y_{CO_2}}{x_{CH_4}/y_{CH_4}}$$

where x_{CO_2} and x_{CH_4} are the CO_2 and CH_4 mole fractions in the adsorbed phase and y_{CO_2} and y_{CH_4} are the CO_2 and CH_4 mole fractions in the bulk phase.

2.2 Computational methods

2.2.1 *Realistic model of disordered porous carbons with heterogeneous chemistry*

The model of disordered porous carbons used in this work, which is shown in Fig. 1, has been obtained using the procedure below (full details can be found in Billemont et al. 2013). We started using the realistic model obtained by Jain et al. (Jain et al. 2005) using a constrained Reverse Monte Carlo method. This model was used in several studies to successfully investigate the effect of disorder on adsorption and freezing in porous materials (Jain et al. 2005; Coasne et al. 2006; Coasne et al. 2007; Coasne et al. 2011). On the other hand, while this model mimics the disordered structure of activated saccharose-based carbon obtained at 1000 °C, it does not contain any oxygen, sulfur, or nitrogen atoms which are responsible for the partial hydrophilicity of real porous carbons. To overcome this limitation, CH and COH groups were added to CS1000A model in order to account for the heterochemistry of real samples (molar ratios H/C = 0.091 and O/C = 0.087) (Jain et al. 2006). We chose to restrict our study to –CH and –COH groups because it allows us to keep the same carbon structure of the original model (which had been developed through a constrained reverse Monte Carlo scheme). We chose not to use –COOH groups for two reasons. First, the experimental sample has more hydrogen atoms than oxygen so that we could not add groups which contain twice as many oxygen than hydrogen (Billemont et al. 2013). Second, CS1000AF has to have the same carbon structure than CS1000A. Thus, in order to include –COOH groups, we would have to find a carbon atom and add both a =O and a –OH bonds. Given the negligible number of carbon atoms in CS1000A for which we can add both a single and a double bond, we decided not to consider –COOH groups. This last argument also holds for –C=O groups. The chemistry of activated carbon is complex so that any realistic model should include all the types of groups above. However, we believe that, because of the lack of information on the chemistry of the system, the simpler description used in the present work is sufficient to demonstrate the effect of surface chemistry on CO_2/CH_4 coadsorption in activated carbons. In what follows, this functionalized model is referred to as CS1000AF. After adding groups to the sample, the system was relaxed by means of Monte Carlo simulations in order to allow the –OH and –H groups to rotate around the carbon atom and find the most favorable configuration. The interaction parameters and partial charges of the groups can be found in our previous work (Billemont et al. 2013).

2.2.2 *Grand Canonical Monte Carlo (GCMC)*

Following previous studies on adsorption and freezing in porous carbons (Coasne et al. 2004; Czwartos et al. 2005), we performed GCMC simulations of nitrogen adsorption at 77 K as well as carbon dioxide and methane coadsorption

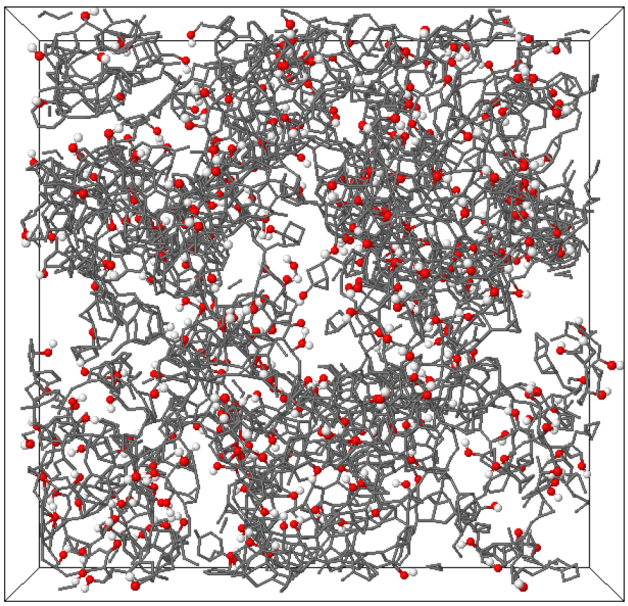

Fig. 1 Molecular configuration of a disordered porous carbon CS1000AF containing –CH and –COH heterogroups. The *sticks* are the C–C, C–H and C–O bonds. *Red* and *white spheres* are the oxygen and hydrogen atoms, respectively. The size of the simulation box is 5 *nm* (Color figure online)

at 318.15 K in CS1000A and CS1000AF. The GCMC technique is a stochastic method that simulates a system having a constant volume V (the pore with the adsorbed phase) in equilibrium with an infinite reservoir of molecules imposing its chemical potential μ_A for each species ($A = CO_2$, CH_4 and N_2) and its temperature T (Frenkel and Smit 2002). The absolute adsorption/desorption isotherm is given by the ensemble average of the number of each adsorbate molecule as a function of the fugacity f_A of the reservoir (the latter are determined from the chemical potential μ_A). While the position of carbon atoms in the porous carbon models are held constant, the –OH and –H groups are allowed to rotate around the carbon which carries them.

All the carbon atoms are described as Lennard-Jones spheres with the following parameters: $\sigma = 0.34$ nm and $\varepsilon = 28$ K (Steele 1973). The rigid model by Harris and Yung was used to describe the carbon dioxide molecule (Harris and Yung 1995). The methane and nitrogen molecules are simply described as single Lennard-Jones spheres (Billemont et al. 2013). The unlike atom Lennard-Jones interaction parameters have been determined using the Lorentz—Berthelot combining rules. The coulombic interaction was computed using the Ewald summation technique. The cut-off distance used to compute the interactions is taken as half the length of the box, $r_c = 2.5$ nm. The parameters of the Ewald summation are $\alpha = 0.128$ and $k_{max} = 7$.

3 Results and discussion

3.1 Characterization of the experimental and numerical samples

Estimating the surface, porosity, and pore size distribution (PSD) requires being able to locate the interface between pore voids and pore walls. To do so, a criterion must be defined although any definition is somewhat arbitrary. Figure 2 shows different possible definitions which allow estimating the pore volume V_{sp}, porosity Φ, and specific surface area S_{sp}. These different definitions can be expressed in terms of different choices for the smallest distance δ between the probe adsorbate molecule and the wall atoms (in what follows, we consider nitrogen as the probe molecule as it corresponds to the most commonly used fluid to characterize porous materials). One can consider the line which corresponds to the contact surface of an adsorbate molecule rolling over the pore surface. The latter definition, which corresponds to Connolly's surface, can be expressed as $\delta = \sigma_{N2-C}/2$. Finally, one can also consider the line which corresponds to the trajectory of the center of mass of an adsorbate molecule as it rolls over the pore surface. Although such a definition, $\delta = \sigma_{N2\text{-}C}$, is supposed to be consistent with the BET surface measured in nitrogen adsorption experiments, they often lead to different specific surfaces due to the fact that the BET method introduces several approximations that are not normally valid for microporous adsorbents. Only specific surfaces obtained using the BET method applied to the experimental and simulated nitrogen adsorption isotherms at 77 K are reported in this work. No geometric specific surfaces have been computed in this work. More details on the effect of the definition used to measure specific surfaces and porous volumes can be found in Coasne and Ugliengo 2012.

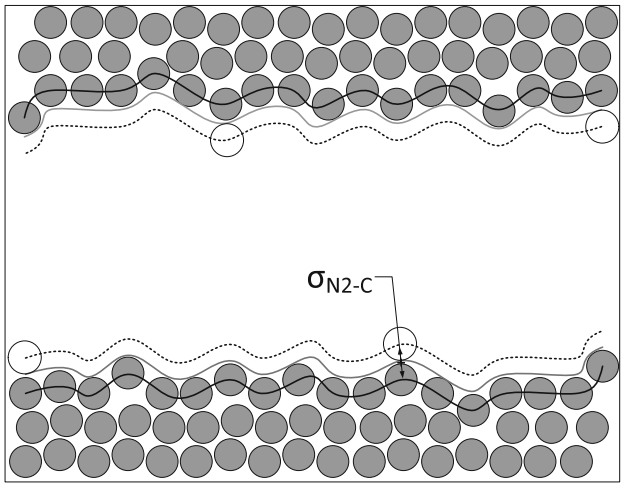

Fig. 2 Definition of the porous volume accessible to an adsorbate. The *black open circles* are adsorbate molecules while the *grey spheres* are the atoms of the porous material. The *black solid line* passes through the center of the atoms at the surface of the pore. The *grey line* corresponds to Connolly's surface, which corresponds to the contact surface of an adsorbate molecule rolling over the surface of the pore. The *dashed line* corresponds to the trajectory of the center of an adsorbate molecule as it rolls over the surface of the pore

Table 1 shows the specific porosity and porous volume estimated for the numerical samples CS1000A and CS1000AF using the different criteria discussed above. The size of the nitrogen molecule $\sigma = 0.36$ nm was used as a reference to test the effect of the criterion.

We also report in Table 1 the porosity of the experimental sample F400. As expected, both the porosity and specific porous volume of the numerical samples decrease upon increasing the size of the probe, i.e. decreasing the region available to the probe. Interestingly, when using the criterion in which the probe cannot approach any wall atom to a distance lower than $\sigma/2$, the porosity and porous volume measured for the numerical samples are similar to those for the experimental sample. In the best case ($\delta = \sigma_{N2}/2$), the specific volume (V_{sp}) determined geometrically by a Monte Carlo scheme overestimates by 15 % the value calculated from the simulated N_2

Table 1 Specific surface areas determined by the BET method (S_{BET}), specific pore volumes (V_p) and specific pore volume (V_{sp}) determined by the BET method, and specific pore volume (V_{sp}) determined by a Monte Carlo procedure with different minimal distances δ between adsorbate atoms and matrix atom centers for the Activated Carbon Sample F400 and the two models, CS1000A and CS1000AF

	CS1000A			CS1000AF			F400
δ	$\sigma_{N2\text{-}C}$	$\sigma_{N2}/2$	$\sigma_{N2\text{-}C}/2$	$\sigma_{N2\text{-}C}$	$\sigma_{N2}/2$	$\sigma_{N2\text{-}C}/2$	–
Porosity (Φ)	0.19	0.63	0.64	0.17	0.58	0.62	0.50
V_{sp} (cm^3/g)	0.26	0.87	0.89	0.21	0.72	0.76	–
S_{BET} (m^2/g)		1601			1408		1150
V_p (cm^3/g)		0.75			0.63		0.61

adsorption isotherm (V_p). V_p is calculated by converting the maximum adsorbed amount into a volume by considering the bulk density of liquid nitrogen at 77 K, 0.808 g/cm^3. The difference between V_{sp} and V_p is thought to be due to this last assumption; indeed, if the true density of confined nitrogen is lower than the bulk density, the above approximation will lead to a value of V_p that underestimates V_{sp}.

This result shows that the numerical samples CS1000A and CS1000AF are reasonable models of the experimental sample in terms of porosity and porous volume. As expected, due to the presence of the heteroatoms in CS1000AF, the porous volume and porosity for this numerical sample are smaller than those for CS1000A.

The PSD of our models CS1000A and CS1000AF can be obtained from their atomic configuration. Following the work of (Gelb and Gubbins 1999), the pore size at a given position in the material can be defined as the diameter of the largest sphere that can be inserted inside the porosity while containing the given position. We used the revised version of the algorithm proposed by Bhattacharya and Gubbins (2006; Bhattacharya et al. 2009) in which the PSD is calculated at random points inside the pore cavity instead of on a grid. Each PSD was calculated by considering 20000 points and the largest sphere for each point was estimated by considering 40000 spheres of various radii. Figure 3 shows the PSD for CS1000A and CS1000AF. As in the case of our estimation of porosity and specific pore volume, two probe sizes were used, $\delta = 0$ and $\delta = \sigma_C/2$. Owing to the fact that CS1000A and CS1000AF share the same carbon backbone, these two samples have very similar PSD. This result shows that the heteroatoms have a negligible effect on the PSD distribution (although data in Table 1 show that they do contribute to reducing the total pore volume and porosity). On the other hand, for both samples, taking into consideration the size of the carbon atoms significantly shifts the PSD to smaller pore sizes. Again, this result shows that the choice of the criterion used to define the PSD and the choice of the probe molecule matter as they lead to different values. Figure 4 shows the nitrogen adsorption isotherm at 77 K for the numerical

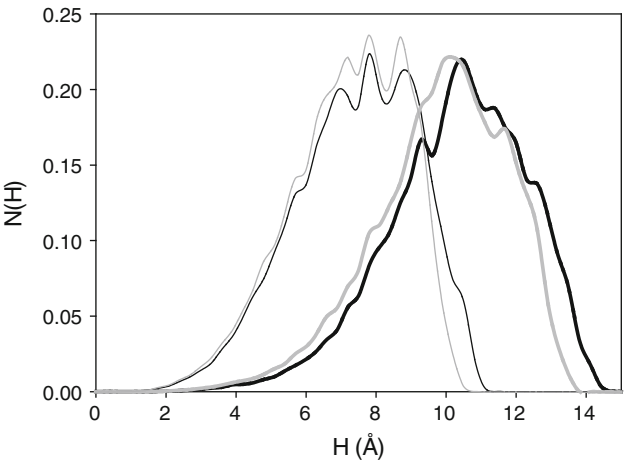

Fig. 3 PSD for CS1000A (black lines) and CS1000AF (grey lines). The *thick lines* show the PSD obtained when considering the centers of carbon atoms only ($\delta = 0$). The *thin lines* are the PSD when considering the extension of the carbon atoms ($\delta = \sigma_C/2$)

samples CS1000A and CS1000AF. The simulated adsorbed amounts of N_2 are obtained as a function of the fugacity in the external phase. In order to compare the experimental and simulated data, the fugacities were converted into pressures using the EOS by Span et al. (2000).

We also show the experimental adsorption isotherm for the sample F400. Both sets of adsorption isotherms are typical of microporous materials (type I—Langmuir adsorption isotherm according to the IUPAC classification). At low pressures, the nitrogen adsorbed amount increases rapidly upon increasing the pressure. Then, as the pores get filled with nitrogen molecules, the adsorbed amount reaches a maximum value which allows estimating the total pore volume (assuming confined nitrogen as a density close to its bulk density). At low pressures, the nitrogen adsorbed amounts are larger for CS1000AF than for CS1000A, owing to enhanced interactions between the nitrogen molecules and the heteroatoms in CS1000AF. In contrast, at higher pressures, the adsorbed amount in CS1000A is slightly larger than in CS1000AF as part of the pore volume in CS1000AF is not available for adsorption because of the presence of the heteroatoms. It should be

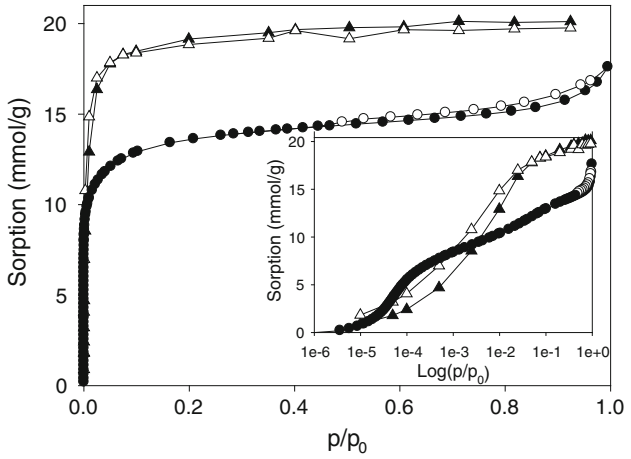

Fig. 4 N_2 adsorption isotherm at 77 K in porous carbons. The circles are experimental data for the Filtrasorb 400 activated carbon (closed and open symbols are the adsorption and desorption data, respectively). The closed and open triangles are the simulated N_2 adsorption isotherms for CS1000A and CS1000AF, respectively. The simulated adsorbed amounts are in *mmol* per *g* of carbon (we omit the mass increase due to addition of heterogroups). Adsorbed amounts for the experimental sample (F400) are in *mmol* per g of sample. p_0 is the bulk saturating vapor pressure for N_2 at 77 K

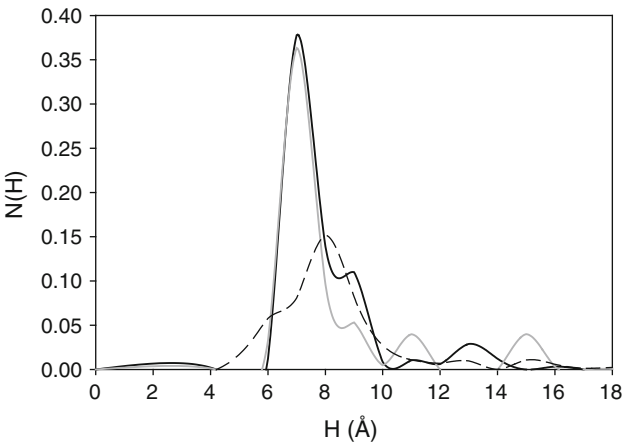

Fig. 5 PSD for CS1000A (*solid black line*), CS1000AF (*solid gray line*), and Filtrasorb 400 (*dashed black line*). These PSD were obtained using the MP method applied to N_2 simulated or experimental adsorption isotherms

noted that the influence of polar sites in CS1000AF on the adsorption of nitrogen is necessarily underestimated because the model used to describe the N_2 molecule does not take into account the quadrupole of the real molecule. We also analyzed the simulated and experimental adsorption isotherms in Fig. 4 using the BET method. For each adsorption isotherm, we also converted the maximum adsorbed amount into a total porous volume (again, assuming confined nitrogen has a density identical to the bulk density, 0.808 g/cm^3). The specific surface area S_{BET} and porous volume V_P for each sample are given in Table 1. Due to the presence of the heteroatoms, which reduce the amount of porous volume accessible to the adsorbate, S_{BET} and V_P for CS1000AF are 12.1 and 15.3 % lower than for CS1000A, respectively. Owing to its higher density compared to those for the numerical samples, the porous volume for F400 is smaller than for CS1000A and CS1000AF.

We also analyzed the experimental and simulated nitrogen adsorption isotherms shown in Fig. 4 using the MP method (Mikhail et al. 1968). This method consists of determining the *t*-plot (Lippens and de Boer 1965) by comparing a N_2 adsorption isotherm with a reference N_2 adsorption isotherm on a similar non-porous material. The MP plot is obtained from the shape of the *t*-plot, which reflects the geometrical heterogeneity of the porous material. Figure 5 shows the PSD for CS1000A, CS1000AF, and F400 as estimated from the MP plot applied to the nitrogen adsorption isotherms in Fig. 4. Again, as observed in the PSD obtained using the geometrical analysis, CS1000A and CS1000AF have very similar PSD as they share the same carbon backbone. The difference between the PSDs for CS1000A and CS1000AF at large pore sizes, i.e. the small peaks at 1.1, 1.3 and 1.5 nm, are due to the sensitivity of the MP-method to the fluctuations in the simulated adsorption isotherms. Moreover, the PSD obtained for these two samples using the MP plot are centered around a value, 0.8 nm, which is consistent with the PSD obtained using the geometrical technique when the size of the carbon atoms is taken into account (Fig. 3). This result further confirms that the choice of the criterion to define the PSD is crucial to accurately predict the PSD relevant to a given application (we recall that there is no universal definition of PSD as it necessarily relies on a choice made to define the extension of the atoms composing the porous material). Interestingly, the PSD of the experimental sample spans over pore sizes which are consistent with those for CS1000A and CS1000AF. This result confirms our previous conclusion that CS1000A and CS1000AF are reasonable models of F400.

3.2 Effect of surface chemistry on carbon dioxide/methane coadsorption and selectivity

In order to estimate the effect of surface chemistry on the coadsorption of mixtures, we performed GCMC simulations of the adsorption of carbon dioxide/methane mixtures in CS1000A and CS1000AF. Figure 6 shows the simulated coadsorption isotherms of carbon dioxide and methane in both samples. We considered different carbon dioxide/methane mixtures with the following molar compositions: 75–25, 50–50, and 25–75 %. The simulated data are obtained with respect to fugacity of the mixture CO_2/CH_4. Again, the fugacities used in the simulations were converted

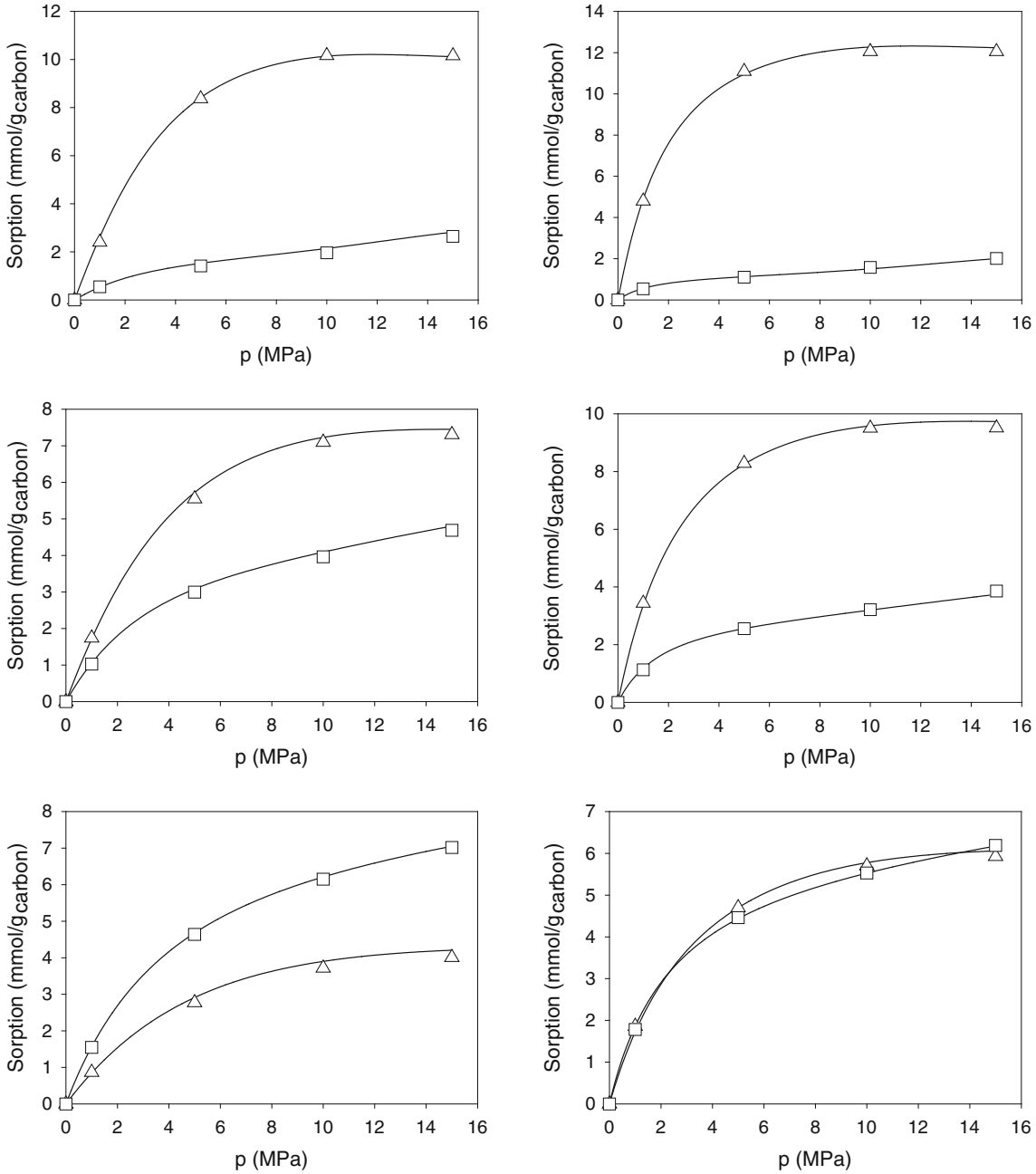

Fig. 6 Simulated coadsorption of carbon dioxide (triangles) and methane (*squares*) at 318.15 K in CS1000A (*left*) and CS1000AF (*right*). The bulk compositions of the carbon dioxide-methane mixture are 75–25 % (*top*), 50–50 % (*middle*) and 25–75 % (*bottom*). The lines are predictions obtained from the simulated pure adsorption isotherms using the equation of Myers and Prausnitz in which only the adsorbed phase is assumed to be ideal (AST)

into total pressures using the EOS by Span and Wagner (1996) for CO_2, the EOS by Setzmann and Wagner (1991) for CH_4, and the mixing rules from Kunz and Wagner (2012).

For all mixture compositions, the coadsorption isotherms are of type I according to the IUPAC classification. The maximum adsorbed amount of carbon dioxide on CS1000A (taken at 15 MPa) is 10.2, 7.3, and 4.0 mmol/g for CO_2 bulk mole fractions of 0.75, 0.5 and 0.25, respectively. The maximum methane adsorbed amounts are 2.6, 4.7, and 7 mmol/g for the same bulk molar compositions. In the case of adsorption on CS1000AF, the adsorbed amounts of CO_2 are higher (12.1, 9.5 and 5.93 mmol/g) and the adsorbed amounts of CH_4 smaller (2, 3.85, 6.2) than on CS1000A. CS1000AF adsorbs more preferentially CO_2 than CS1000A, due to the fact the heterogroups in CS1000AF have stronger interactions with CO_2 than CH_4

(because of the quadrupole of CO_2). This appears more clearly on the values of the selectivity of the adsorbent for CO_2 relative to CH_4 given in Table 2. These selectivities vary from 1.28 to 1.97 for CS1000A and from 1.99 to 3.35 for CS1000AF. We thus conclude that the presence of heterogroups on carbon porous materials has a significant effect on the coadsorption of CO_2 and CH_4 and, hence, must be taken into account. For example, the CO_2 adsorbed amount is always higher or equal to the CH_4 adsorbed amount in CS1000AF (Fig. 6).

Table 2 Selectivities of the adsorbents for carbon dioxide with respect to methane for different carbon dioxide bulk mole fractions. Different total pressures are considered: 1, 5 and 15 MPa

$S_{CO2,CH4}$				
p (MPa)	y_{CO2}	CS1000A	F400	CS1000AF
1	0.75	1.47	3.16	2.96
	0.5	1.69	3.06	3.04
	0.25	1.68	2.96	3.13
5	0.75	1.97	3.78	3.35
	0.5	1.85	3.69	3.24
	0.25	1.79	3.55	3.16
15	0.75	1.28	–	1.99
	0.5	1.56	–	2.47
	0.25	1.71	–	2.87

Figure 6 also shows the predictions obtained using the adsorbed solution theory (AST) with pure CO_2 and CH_4 adsorption isotherms (Myers and Prausnitz, 1965). AST is a less restrictive version of the well-known Ideal Adsorbed Solution Theory (IAST) in which the adsorbed and gas phases are not assumed to be ideal phases. The latter theory describes the equilibrium between the gas phase and the adsorbed phase given by (Myers and Prausnitz 1965):

$$py_i\phi_i = f_i^0(\pi)\gamma_i x_i \quad (\text{constant}T) \tag{2}$$

where p is the total pressure of the gas phase, y_i and x_i are the mole fraction of component i in the gas and adsorbed phase, respectively. ϕ_i and γ_i are the fugacity and activity coefficients, respectively. $f_i^0(\pi)$ is the fugacity of pure adsorbate i at the temperature and spreading pressure (π) of

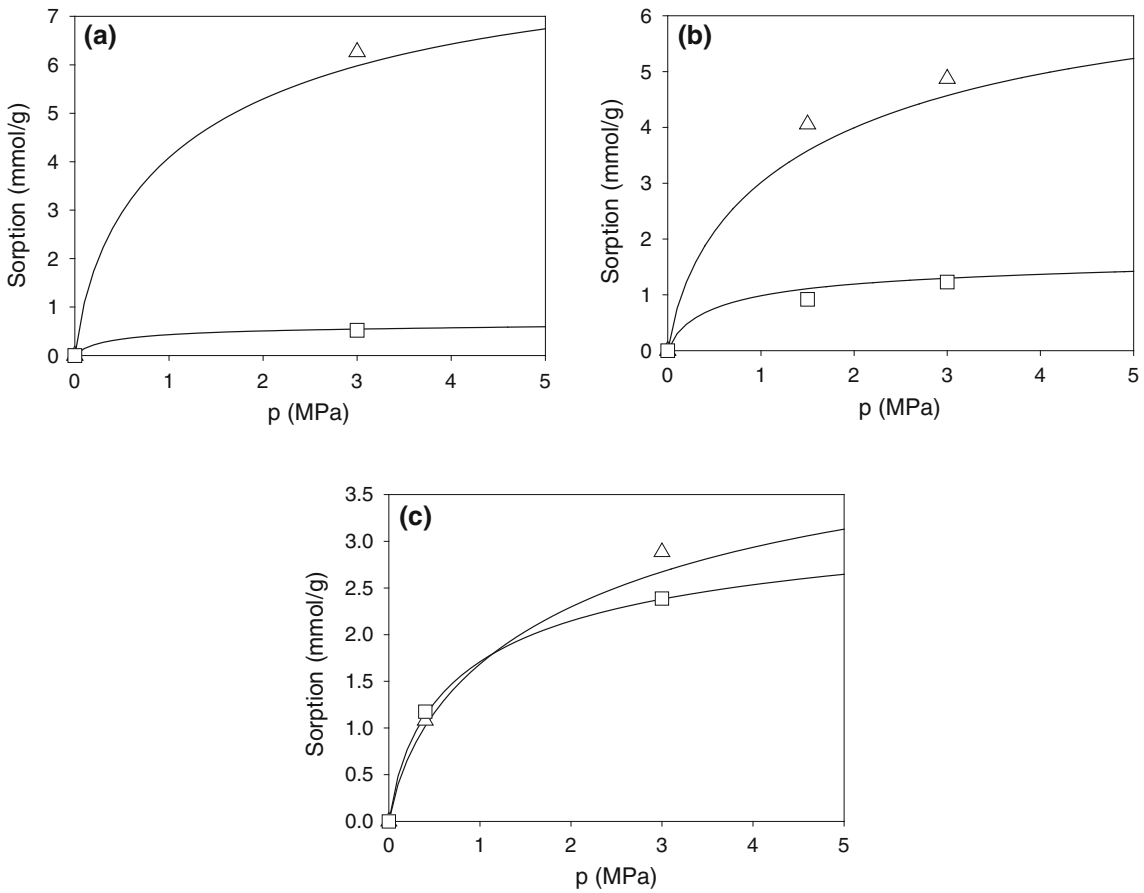

Fig. 7 Experimental coadsorption isotherms for carbon dioxide (*triangles*) and methane (*squares*) at 318.15 K in Filtrasorb 400 activated carbon.The bulk compositions of the carbon dioxide-methane mixture are 75–25 % (**a**), 50–50 % (**b**) and 25–75 % (**c**). The lines are predictions obtained from the experimental pure adsorption isotherms using the equation of Myers and Prausnitz in which only the adsorbed phase is assumed to be ideal (AST)

the mixture, i.e. in the standard state. For details about the calculations, the reader is referred to original publications on AST or to our paper (Billemont et al. 2013). The fugacity coefficients are determined from the carbon dioxide EOS by (Span and Wagner 1996), the methane EOS by (Setzmann and Wagner 1991), and the mixing rules by (Kunz and Wagner 2012). The activity coefficients are taken equal to 1 as we consider that the adsorbed phase behaves as an ideal phase. As shown in Fig. 6, the molecular simulations and the predictions based on AST are in good agreement. The discrepancy observed between the simulated and theoretical data can be attributed to the fact that the theory assumes that the adsorbed phase is an ideal adsorbed phase with no interaction.

Figure 7 shows the experimental coadsorption isotherms of carbon dioxide and methane in F400. As in the case of the simulations, we considered carbon dioxide/methane mixtures with the following molar compositions: 75–25, 50–50, and 25–75 %. Owing to the fact that the numerical and experimental samples have different porous volumes, a quantitative comparison between these samples is not relevant. However, for all mixture compositions, the experimental coadsorption isotherms, which are of type I according to the IUPAC classification, resemble those observed in the simulations.

The simulated data for CS1000AF better agree with the experimental data than those for CS1000A. This result is confirmed by the selectivities given in Table 2; the discrepancy between the simulated and experimental selectivities varies from 43 to 54 % for CS1000A and from 0.7 to 12 % for CS1000AF. This result shows that it is necessary to take into account the surface chemistry of the porous carbon in order to simulate in a realistic fashion the coadsorption of CO_2 and CH_4. This conclusion is consistent with previous works (Jorge and Seaton 2003; Nicholson and Gubbins 1996). Jorge and Seaton studied the adsorption of hydrocarbon-water mixtures on an activated carbon modeled by an assembly of slit-pores containing carboxyl groups. The authors showed the importance of the distribution of these groups on pores of different sizes. This result is consistent with the work by Nicholson and Gubbins who showed that the pore size is not sufficient to predict coadsorption of CO_2/CH_4 mixtures in carbons. The interactions between adsorbed molecules, and between adsorbed molecules and adsorbent also influence the selectivity. (Nicholson and Gubbins 1996).

We also compare in Fig. 7 the predictions obtained using the AST and the experimental coadsorption isotherms. As in the case of the simulated data, the theoretical coadsorption isotherms were predicted on the basis of the adsorption isotherms for pure CO_2 and CH_4. The experimental data and the predictions based on AST are in good agreement. This result suggests that carbon storage and methane recovery in coals can be predicted using AST without having to conduct numerous tedious experiments of gas mixture adsorption.

4 Conclusion

This paper reports a joint experimental and molecular simulation study of the coadsorption of CO_2 and CH_4 in porous carbons. As far as molecular simulation is concerned, we address the effect of surface chemistry by considering a disordered model of porous carbons which has been modified to include heterogroups. The experimental and numerical samples are first compared in terms of PSD, specific surface area, porous volume, and porosity. We also discuss the different criteria used to estimate the latter properties from a geometrical analysis. We show that the numerical samples used in this work are reasonable models to describe gas adsorption in real samples. As an important result of the present work, we demonstrate the ability of the MP method to estimate the PSD of porous carbons from nitrogen adsorption isotherms. Both the experimental and simulated coadsorption isotherms resemble those obtained for pure gases (type I—Langmuir in the IUPAC classification). We show that the surface chemistry has an important effect on the selectivity of the adsorbent and that it should be taken into account to simulate adequately the coadsorption of CO_2 and CH_4. The simulated and experimental coadsorption isotherms are well described by the AST. As a result, thanks to this theory in which no adjustment is required (the coadsorption isotherm is directly estimated from adsorption measurements for pure fluids), accurate prediction can be made without having to measure a large number of coadsorption isotherms.

References

Aaron, D., Tsouris, C.: Separation of CO2 from flue gas: a Review. Sep. Sci. Technol **40**, 321–348 (2005)

Bae, J.S., Bhatia, S.K.: High-pressure adsorption of methane and carbon dioxide on coal. Energy Fuels **20**, 2599–2607 (2006)

Bhattacharya, S., Coasne, B., Hung, F.R., Gubbins, K.E.: Modeling micelle-templated mesoporous material SBA-15: atomistic model and gas adsorption studies. Langmuir **25**, 5802–5813 (2009)

Bhattacharya, S., Gubbins, K.E.: Fast method for computing pore size distributions of model materials. Langmuir **22**, 7726–7731 (2006)

Billemont, P., Coasne, B., De Weireld, G.: An experimental and molecular simulation study of the adsorption of carbon dioxide and methane in nanoporous carbons in the presence of water. Langmuir **27**, 1015–1024 (2011)

Billemont, P., Coasne, B., De Weireld, G.: Adsorption of carbon dioxide, methane, and their mixtures in porous carbons: effect of

surface chemistry, water content, and pore disorder. Langmuir **29**, 3328–3338 (2013)
Brochard, L., Vandamme, M., Pellenq, R.J.M.: Poromechanics of microporous media. J. Mech. Phys. Solids **60**, 606–622 (2012a)
Brochard, L., Vandamme, M., Pellenq, R.J.M., Fen-Chong, T.: Adsorption-induced deformation of microporous materials: coal swelling induced by co2–ch4 competitive adsorption. Langmuir **28**, 2659–2670 (2012b)
Busch, A., Gensterblum, Y., Krooss, B.M., Littke, R.: Methane and carbon dioxide adsorption–diffusion experiments on coal: upscaling and modeling. Int. J. Coal Geol **60**, 151–168 (2004)
Chen, G., Yang, J., Liu, Z.: Method for simultaneous measure of sorption and swelling of the block coal under high gas pressure. Energy Fuels **26**, 4583–4589 (2012)
Clauzier, S., Ho, L.N., Pera-Titus, M., Coasne, B., Farrusseng, D.: Enhanced H_2 uptake in solvents confined in mesoporous metal–organic framework. J. Am. Chem. Soc **134**, 17369–17371 (2012)
Coasne, B., Alba-Simionesco, C., Audonnet, F., Dosseh, G., Gubbins, K.E.: Adsorption and structure of benzene on silica surfaces and in nanopores. Langmuir **25**, 10648–10659 (2009)
Coasne, B., Alba-Simionesco, C., Audonnet, F., Dosseh, G., Gubbins, K.E.: Adsorption, structure and dynamics of benzene in ordered and disordered porous carbons. Phys. Chem. Chem. Phys **13**, 3748–3757 (2011)
Coasne, B., Czwartos, J., Gubbins, K.E., Hung, F.R., Sliwinska-Bartkowiak, M.: Freezing and melting of binary mixtures confined in a nanopore. Mol. Phys **102**, 2149–2163 (2004)
Coasne, B., Czwartos, J., Gubbins, K.E., Hung, F.R., Sliwinska-Bartkowiak, M.: Freezing of mixtures confined in a slit nanopore. Adsorption **11**, 301–306 (2005)
Coasne, B., Jain, S., Gubbins, K.: Adsorption, structure and dynamics of fluids in ordered and disordered models of porous carbons. Mol. Phys **104**, 3491–3499 (2006)
Coasne, B., Jain, S.K., Naamar, L., Gubbins, K.E.: Freezing of argon in ordered and disordered porous carbon. Phys. Rev. B **76**, 085416 (2007)
Coasne, B., Ugliengo, P.: Atomistic model of micelle-templated mesoporous silicas: structural, morphological, and adsorption properties. Langmuir **28**, 11131–11141 (2012)
Cui, X., Bustin, R.M., Chikatamarla, L.: Adsorption-induced coal swelling and stress: implications for methane production and acid gas sequestration into coal seams. J. Geophys. Res **112**, B10202 (2007)
Czwartos, J., Coasne, B., Gubbins, K.E., Hung, F.R., Sliwinska-Bartkowiak, M.: Freezing and melting of azeotropic mixtures confined in nanopores: experiment and molecular simulation. Mol. Phys **103**, 3103–3113 (2005)
Day, S., Duffy, G., Sakurovs, R., Weir, S.: Effect of coal properties on CO_2 sorption capacity under supercritical conditions. Int. J. Greenhouse Gas Control **2**, 342–352 (2008)
Frenkel, D., Smit, B.: Understanding molecular simulation : from algorithms to applications, 2nd edn. Academic, San Diego; London (2002)
Gelb, L.D., Gubbins, K.E.: Pore size distributions in porous glasses: a computer simulation study. Langmuir **15**, 305–308 (1999)
Gensterblum, Y., van Hemert, P., Billemont, P., Battistutta, E., Busch, A., Krooss, B.M., De Weireld, G., Wolf, Khaa: European inter-laboratory comparison of high pressure co2 sorption isotherms ii: natural coals. Int. J. Coal Geol. **84**, 115–124 (2010)
Gensterblum, Y., van Hemert, P., Billemont, P., Busch, A., Charriére, D., Li, D., Krooss, B.M., de Weireld, G., Prinz, D., Wolf, K.H.A.A.: European inter-laboratory comparison of high pressure CO2 sorption isotherms. I: activated carbon. Carbon **47**, 2958–2969 (2009)
Goodman, A.L., Busch, A., Bustin, R.M., Chikatamarla, L., Day, S., Duffy, G.J., Fitzgerald, J.E., Gasem, K.A.M., Gensterblum, Y., Hartman, C., Jing, C., Krooss, B.M., Mohammed, S., Pratt, T., Robinson Jr, R.L., Romanov, V., Sakurovs, R., Schroeder, K., White, C.M.: Inter-laboratory comparison II: cO2 isotherms measured on moisture-equilibrated Argonne premium coals at 55 °C and up to 15 MPa. Int. J. Coal Geol **72**, 153–164 (2007)
Harris, J.G., Yung, K.H.: Carbon dioxide's liquid-vapor coexistence curve and critical properties as predicted by a simple molecular model. J Phy Chem **99**, 12021–12024 (1995)
Heymans, N., Alban, B., Moreau, S., De Weireld, G.: Experimental and theoretical study of the adsorption of pure molecules and binary systems containing methane, carbon monoxide, carbon dioxide and nitrogen. Application to the syngas generation. Chem. Eng. Sci **66**, 3850–3858 (2011)
Hildenbrand, A., Krooss, B., Busch, A., Gaschnitz, R.: Evolution of methane sorption capacity of coal seams as a function of burial history—a case study from the Campine Basin NE Belgium. Int. J. Coal Geol **66**, 179–203 (2006)
Ho, L.N.: Perez Pellitero, J., Porcheron, F., Pellenq, R.J.M.: enhanced CO2 Solubility in Hybrid MCM-41: Molecular Simulations and Experiments. Langmuir **27**, 8187–8197 (2011)
Jain, S.K., Pikunic, J.P., Pellenq, R.J.M., Gubbins, K.E.: Effects of activation on the structure and adsorption properties of a nanoporous carbon using molecular simulation. Adsorption **11**, 355–360 (2005)
Jain, S.K., Pellenq, R.J.M., Pikunic, J.P., Gubbins, K.E.: Molecular modeling of porous carbons using the hybrid reverse Monte Carlo method. Langmuir **22**(24), 9942–9948 (2006)
Jorge, M., Seaton, N.A.: Predicting adsorption of water/organic mixtures using molecular simulation. AIChE J. **49**(8), 2059–2070 (2003). doi:10.1002/aic.690490815
Kaul, B.K.: A modern version of volumetric apparatus for measuring gas-solid equilibrium data. Ind. Eng. Chem. Res **26**, 928–933 (1987)
Kunz, O., Wagner, W.: The GERG-2008 wide-range equation of state for natural gases and other mixtures: An expansion of GERG-2004. J. Chem. Eng, Data (2012)
Lewis, W.K., Gilliland, E.R., Chertow, B., Cadogan, W.P.: Adsorption equilibria hydrocarbon gas mixtures. Ind. Eng. Chem **42**, 1319–1326 (1950)
Lippens, B.C., de Boer, J.H.: Studies on pore systems in catalysts: V. t method. J. Catal. **4**, 319–323 (1965)
Mathews, J.P., van Duin, A., Chaffee, A.: The utility of coal molecular models. Fuel Proc. Technol **92**, 718–728 (2011)
Mathews, J.P., Chaffee, A.: The molecular representations of coal—a review. Fuel **96**, 1–14 (2012)
Mazzotti, M., Pini, R., Storti, G.: Enhanced coalbed methane recovery. J Supercrit. Fluids **47**, 619–627 (2009). doi:10.1016/j.supflu.2008.08.013
Metz, B., Davidson, O., De Coninck, H., Loos, M., Meyer, L.: IPCC special report on carbon dioxide capture and storage. In. Intergovernmental Panel on Climate Change, Geneva (Switzerland). Working Group III, (2005)
Mikhail, R.S., Brunauer, S., Bodor, E.E.: Investigations of a complete pore structure analysis: I. Analysis of micropores. J. Colloid Interface Sci **26**, 45–53 (1968)
Myers, A.L., Prausnitz, J.M.: Thermodynamics of mixed-gas adsorption. AIChE J **11**, 121–127 (1965). doi:10.1002/aic.690110125
Nicholson, D., Gubbins, K.E.: Separation of carbon dioxide–methane mixtures by adsorption: effects of geometry and energetics on selectivity. J. Chem. Phys **104**(20), 8126–8134 (1996)
Ottiger, S., Pini, R., Storti, G., Mazzotti, M., Bencini, R., Quattrocchi, F., Sardu, G., Deriu, G.: Adsorption of pure carbon dioxide and methane on dry coal from the Sulcis Coal Province (SW Sardinia, Italy). Environ. Prog **25**, 355–364 (2006)
Setzmann, U., Wagner, W.: A new equation of state and tables of thermodynamic properties for methane covering the range from

the melting line to 625 K at pressures up to 1000 MPa. J. Phys. Chem. Ref. Data **20**, 1061–1155 (1991)

Span, R., Lemmon, E.W., Jacobsen, R.T., Wagner, W., Yokozeki, A.: A reference equation of state for the thermodynamic properties of nitrogen for temperatures from 63.151 to 1000 k and pressures to 2200 Mpa. J. Phys. Chem. Ref. Data **29**(6), 1361–1433 (2000)

Span, R., Wagner, W.: A New equation of state for carbon dioxide covering the fluid region from the triple-point temperature to 1100 K at pressures up to 800 MPa. J. Phys. Chem. Ref. Data **25**, 1509–1596 (1996)

Steele, W.A.: The physical interaction of gases with crystalline solids: I. Gas-solid energies and properties of isolated adsorbed atoms. Surf. Sci **36**, 317–352 (1973)

Tambach, T.J., Mathews, J.P., van Bergen, F.: Molecular exchange of CH4 and CO2 in Coal: enhanced coalbed methane on a nanoscale. Energy Fuels **23**, 4845–4847 (2009)

Tenney, C., Lastoskie, C.: Molecular simulation of carbon dioxide adsorption in chemically and structurally heterogeneous porous carbons. Environ. Prog **25**, 343–354 (2006)

White, C.M., Smith, D.H., Jones, K.L., Goodman, A.L., Jikich, S.A., LaCount, R.B., DuBose, S.B., Ozdemir, E., Morsi, B.I., Schroeder, K.T.: Sequestration of carbon dioxide in coal with enhanced coalbed methane recovery a review. Energy Fuels **19**, 659–724 (2005)